CORA Cork Open Research Archive
Cartlann Taighde Oscailte Chorcaí

Title	Dependence of current on porous layer structure during anodization of n-InP in aqueous KOH electrolytes
Authors	Lynch, Robert P.;Quill, Nathan;O'Dwyer, Colm;Buckley, D. Noel
Publication date	2013-07-01
Original Citation	Lynch, R. P., Quill, N., O'Dwyer, C. and Buckley, D. N. (2013) 'Dependence of Current on Porous Layer Structure during Anodization of n-InP in Aqueous KOH Electrolytes', ECS Transactions, 50(37), pp. 191-203. doi: 10.1149/05037.0191ecst
Type of publication	Article (peer-reviewed)
Link to publisher's version	http://ecst.ecsdl.org/content/50/37/191.abstract - 10.1149/05037.0191ecst
Rights	© 2013 ECS - The Electrochemical Society
Download date	2026-10-31 03:16:11
Item downloaded from	https://hdl.handle.net/10468/6161



UCC
University College Cork, Ireland
Coláiste na hOllscoile Corcaigh

Dependence of Current on Porous Layer Structure during Anodization of n-InP in Aqueous KOH Electrolytes

Robert P. Lynch, Nathan Quill, Colm O'Dwyer,[a] and D. Noel Buckley

Materials and Surface Science Institute, and Department of Physics and Energy, University of Limerick, Limerick, Ireland
[a] *Department of Chemistry, University College Cork, Cork, Ireland and Micro & Nanoelectronics Centre, Tyndall National Institute, Lee Maltings, Cork, Ireland*

We have performed a computer simulation of the current during anodization of InP in aqueous KOH electrolyte based on the spatial characteristics of the porous structures that are formed. Specifically, we have developed a model, based on the expansion and merging of the porous domains and compared current densities during linear potential sweep and potentiostatic experiments to their respective simulated current-density data. Furthermore, we have compared the expected pore structure at particular stages of etching with corresponding micrographs. From these investigations we are able to demonstrate how the porous structure influences the observed current density.

INTRODUCTION

The variety of semiconductors that can be rendered porous electrochemically includes Si,[1,2] GaAs,[3,4] InP,[5-13] GaP [14] and many others. When an anodic potential is applied to an n-type semiconductor, the material near the surface becomes depleted of carriers. This region of fixed space charge prevents etching since the semiconductor is unable to conduct carriers to the electrolyte interface. Where defects arise on the electrode surface, variations in the energy levels of the surface state (perhaps due to defects and surfaces ledges) or variations in the space charge layer width (perhaps due to a local perturbation of the doping density) can allow localized etching to occur.[6] This localized etching leads to the formation of surface pits. At these pits the electric field is magnified due to the high surface-curvature of the pit walls.[15] Under these conditions quantum tunneling of holes from the valence band, due to the pits acting as centers of high electric-field, results in increased localized etching at the surface pits.

Previous work by our group [16-22] showed that porous structures are obtained when InP is anodized in aqueous KOH at concentrations of 2 mol dm^{-3} or greater.[17] This porosity originates from pits in the surface creating domains of pores beneath a thin (~40 nm) dense near-surface layer of InP.[18] The pores in these domains propagate preferentially along the <111>A crystallographic directions.[16] Therefore, the domains that initially form have triangular $(01\bar{1})$ cross-sections, 'dove-tail' (011) cross-sections and rectangular profiles when viewed in (100) planes parallel to the electrode surface.[17] Each domain is connected to the surface via an individual channel, and eventually these domains merge to form a continuous porous layer, beneath the near-surface layer.[18,20]

In this paper, the variations in current density observed in linear potential sweep (LPS) and potentiostatic experiments during which n-InP is anodized in aqueous KOH electrolyte are described. A mathematical model of pore growth – based on the expansion

and merging of truncated tetrahedral porous domains – is developed and the reasons behind the variations in current in the model are described. Scanning-electron-microscopy (SEM) images of samples that have been etched for different durations are investigated so as to surface-pit density and the porous structure beneath the surfaces after different durations of etching. The results from SEM investigations are compared to the initial current vs. time behavior of potentiostatic and LPS experiments and these comparisons are used to verify our model.

EXPERIMENTAL

The working electrode consisted of polished (100)-oriented monocrystalline sulfur-doped n-type InP. An ohmic contact was made to the back of the InP sample and isolated electrically from the electrolyte by means of a suitable varnish. The electrode area was typically 0.2 cm^2. InP wafers with carrier concentrations from 5.3-6.7 $\times 10^{18}$ cm^{-3} and etch pit densities < 5000 cm^{-2} were used. Anodization was carried out in aqueous KOH electrolytes of 5 mol dm^{-3}. Each linear potential sweep (LPS) experiment was performed at 2.5 mV s^{-1} from 0.0 V (SCE) to a predefined upper potential. Alternatively, potentiostatic experiments were performed for a predefined duration.

A conventional three-electrode cell configuration was used employing a platinum counter electrode and a saturated calomel reference electrode (SCE) to which all potentials were referenced. Prior to immersion in the electrolyte, the working electrode was dipped in an etchant (3:1:1 H_2SO_4:H_2O_2:H_2O) for 4 minutes and then rinsed in deionized water. All of the electrochemical experiments were carried out in the absence of light at room temperature.

A CH Instruments Model 650A Electrochemical Workstation was employed for cell parameter control and for data acquisition. Cleaved {011} cross-sections were examined using a HITACHI S-4800 field emission SEM operating at 5 kV.

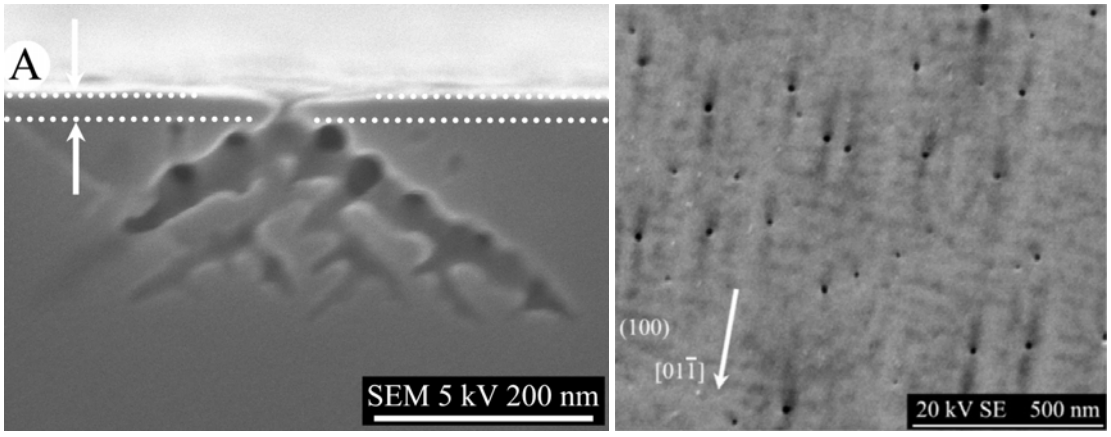
RESULTS AND DISCUSSION

Pits start to form in the surface of InP anodized in KOH once the potential being applied is greater than a characteristic threshold potential. These pits are the origin of pore growth (see Fig. 1). Pores spread into the bulk semiconductor from these pits, leaving an almost intact near-surface layer of dense InP (Fig. 1a at A). Each pit therefore produces an individual domain of pores that are linked back through it to the surface.

Figure 2 shows a linear sweep voltammogram (LSV). Two peaks in current – the first at 0.252 V (V_1) and the second at 0.383 V (V_2) – can be observed. Initially (*i.e.* prior to 0.15 V) no significant porous etching is observed as verified by SEM images of the surfaces of samples etched for such limited durations (images not shown). However, for samples that have undergone LPS experiments to upper potentials greater than 0.15 V, pits in the electrode surface (similar to those in Fig. 1b) and domains of pores that extend from them into the bulk of the electrode (as shown in Fig. 1a) are observed.

The surface-pit density is also plotted against potential in Fig. 2. The density of surface pits at a given potential was obtained by performing an LPS as far as that potential and then examining the surface using SEM. The density of pits continues to increase as potential increases (and time passes) until the surface pit density saturates at a potential in the vicinity of V_1 and V_T: the potential of the first peak in current and the

potential corresponding to a trough in current after V_1, respectively. After V_T the number of surface pits is independent of the applied potential and there is an almost linear increase of current with potential.



(a) (b)

Fig. 1 (a) SEM micrograph of (011) cleavage plane following a LPS from 0.0 to 0.245 V (SCE) ($n = 5.3 \times 10^{18}$ cm^{-3}) showing the cross-sections of a young porous domain that has not yet merged, growing from a pit in the surface beneath a near-surface layer (at A). (b) SEM micrograph of an InP (100) surface ($n = 3.4 \times 10^{18}$ cm^{-3}) following an LPS from 0.0 to 0.537 V (SCE). Since the image was taken at 20 kV both the surface pits and some sub-surface features are shown.

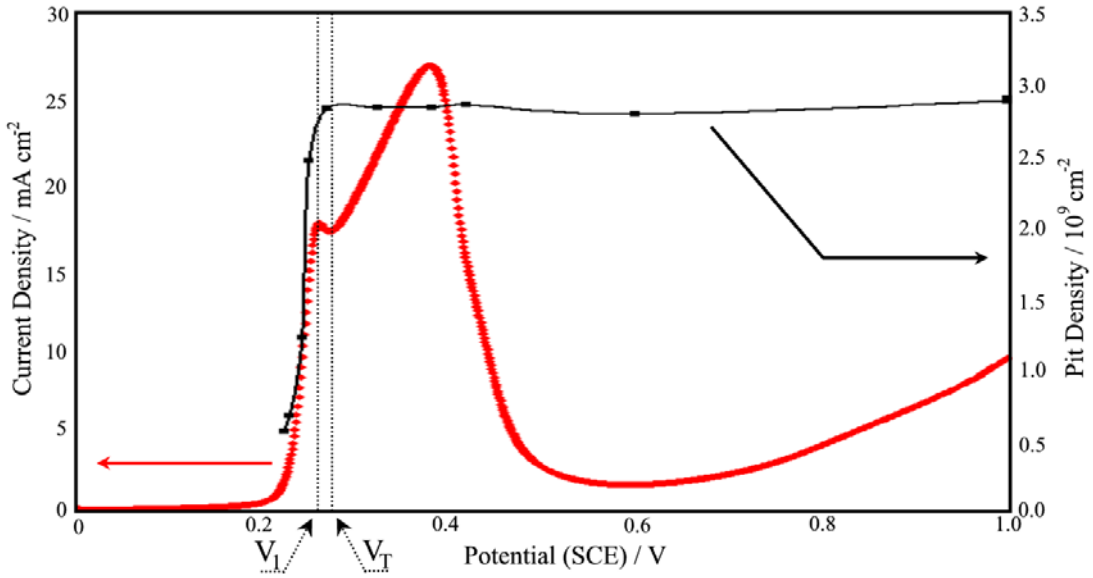


Fig. 2 Linear sweep voltammogram and surface pit density versus potential for InP (n = 5 to 5.6 x 10^{18} cm^{-3}) from 0 to 1.0 V (SCE) at 2.5 mV s^{-1} in 5 mol dm^{-3} KOH.

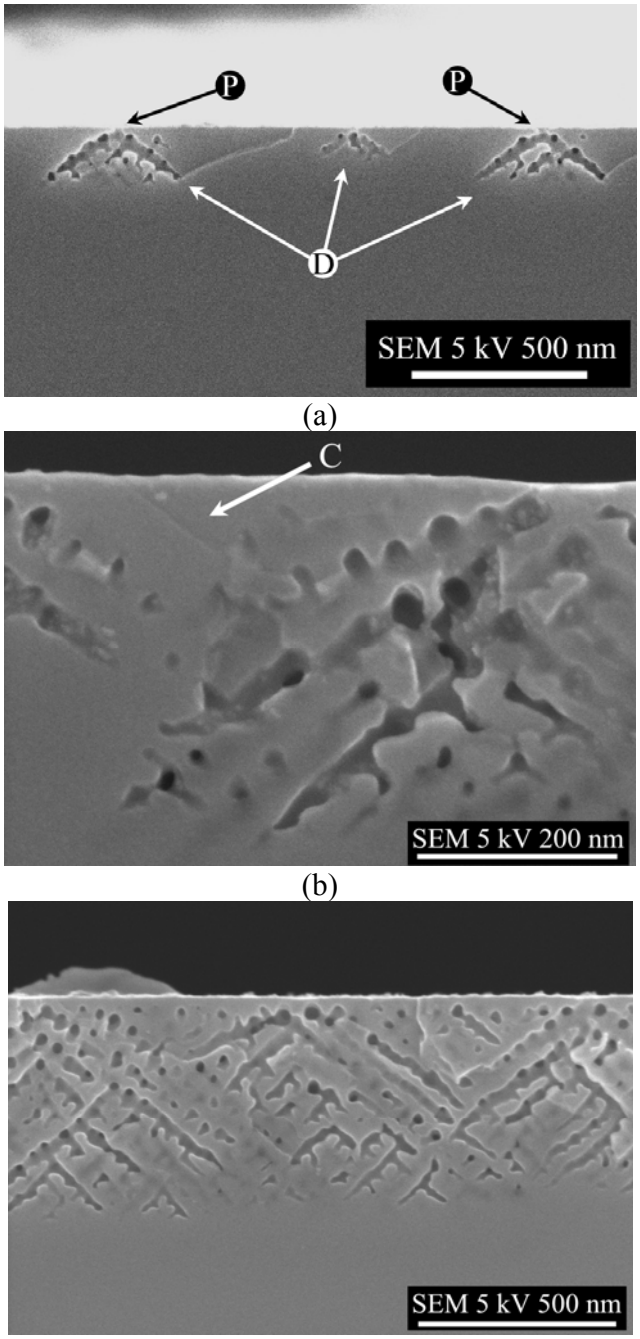


Fig. 3 SEM micrograph of (011) cleavage plane of n-InP following an LPS from 0.0 to (a) 0.245 V (SCE) (just before 1st current peak), (b) 0.252 V (SCE) (1st current peak) and (c) 0.27 V (SCE) (small trough after 1st current peak) (n = 5 to 5.6 × 10^{18} cm^{-3}). (a) The cross-sections of porous domains that have not begun to merge, (b) that have begun to merge but have not completed the process – *i.e.* there is a non-porous region visible at C – and (c) that have merged fully into one continuous layer are observed.

SEM Investigation of Pitting and Pore Propagation during First Current Peak

Figure 3 shows SEM (011) cross-section images of porous layers after LPSs from 0 to 0.245 V, 0.252 V and 0.27 V which correspond to a potential just below V_1, at V_1 and at V_T (*i.e.* before, at and after the peak in current), respectively. In Fig. 3a (image of sample prior to V_1) merging of domains has not proceeded to a significant extent and three isolated domain cross-sections (at D), along with their surface-pits (at P) can be seen in the image. In Fig. 3b (image of sample at V_1) two domain cross-sections can be partially observed. Although merging of domains has already started some of the regions between the merging domains and the electrode surface, as seen at C, are not porous *i.e.* the porous domains have not merged fully. Figure 3c (image of a sample at V_T) shows several different domains *i.e.* pores growing from several different origins. These domains have merged fully together to form a continuous layer where the pores have filled all the gaps between the porous domains and the dense near-surface layer. At this stage the near-surface layer of dense InP is isolated from the bulk InP.

From this analysis of cross-sectional SEM images it can be concluded that isolated domains exist prior to V_1 (*i.e.* the first current peak) while after the trough in current at V_T all the domains are found to be merged into one continuous porous layer. Therefore the first current peak corresponds to the merging of domains. As will be shown later, the decrease in current is primarily due to the decrease in the number of active pore tips as the merging process is completed between V_1 and V_T, after which the number of active tips is maintained at a steady-state value.

In Fig. 2 saturation of surface pit density occurs in the vicinity of V_1 and V_T. It is to be expected that saturation in pit density should occur as domain merging is completed (*i.e.* at V_T), since the formation of pits is dependent on the availability of carriers from bulk InP that can transfer across the depletion layer near the electrode surface to the electrode-electrolyte interface. Therefore when the domains begin to merge together, the carrier-depleted near-surface layer can only be etched in the regions where the domains do not exist beneath the surface. It follows, that as domains grow the area where carriers are available beneath the electrode surface reduces resulting in a shrinking of the regions of the electrode surface where pit formation can occur. Eventually when the domains merge fully (*i.e.* at V_T) the near-surface layer becomes fully isolated from the substrate (*i.e.* bulk InP) by a porous layer which is depleted of carriers, resulting in the saturation of pit density. Therefore, the initial rise in current is both due to the increase in pit density (*i.e.* increase in the overall number of domains) at the surface and the expansion of each porous domain (*i.e.* increase in the number of active pore tips per domain) beneath the surface. Furthermore, the current reaches a maximum value and then falls off slightly when the surface pit density reaches a maximum and the porous domains merge into a continuous porous-layer, *i.e.* when the number of active pore tips reaches a steady-state value.

Model of Domain Merging

The charge required to grow a specific depth of continuous porous layer can be calculated from SEM and LSV data. Therefore, if the domain shape of the pores growing from an individual surface pit is taken to be a truncated tetrahedron [17] (schematically depicted in Fig. 4) it is possible to calculate the current required to etch such a domain. Assuming most of the variations can be accounted for by the expansion and merging of porous domains (and not from the formation of new surface pits), multiplying the current

required to grow an average domain by the maximum surface pit density (*i.e.* the surface pit density after V_T) allows the expected current density to be calculated. Since this is equivalent to the current density during initial etching it follows that a theoretical current versus time graph for the initial period of etching can be constructed.

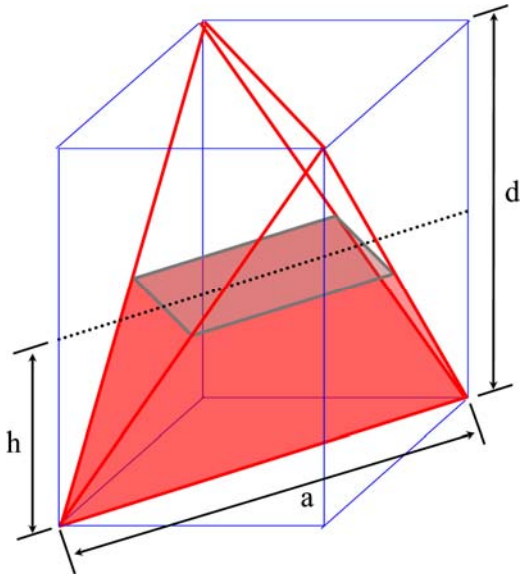


Fig. 4 Tetrahedron enclosed by a cube of side d. The lower half of the tetrahedron represents the overall volume of an individual porous domain.

In the schematic in Fig. 4 the lower half of the tetrahedron corresponds to the domain shape for a (100)-oriented electrode surface and its volume V_D is

$$V_D = \frac{d^3}{6} \qquad [1]$$

where d is the length of the side of the cube within which the tetrahedron is drawn. Since charge Q is proportional to volume etched (*i.e.* V_D) the current i must be proportional to the derivative of volume with respect to time: *i.e.*

$$Q = \frac{nF}{V_M} \times V_D \qquad [2]$$

$$i = \frac{dQ}{dt} = \frac{nF}{V_M} \times \frac{d(V_D)}{dt} \qquad [3]$$

where n is the number of electrons required to etch one mole of InP, V_M is its molar volume and F is the Faraday constant. As mentioned above the current density j of an experiment can be calculated by multiplying the current per domain i by the maximum surface-pit density ρ. Therefore the charge density q and current density j for the overall electrode surface can be calculated:

$$q = \frac{\rho nF}{V_M} \times V_D \qquad [4]$$

$$j = \frac{dQ}{dt} = \frac{\rho nF}{V_M} \times \frac{d(V_D)}{dt} \qquad [5]$$

When an isolated domain merges with other domains its volume V_D can no longer expand at the same rate. The excluded volumes (*i.e.* the volumes of the regions that a

domain can no longer expand into, but would have if it were an isolated domain) can be calculated (see Appendix A). Thus, the volume of the average domain can be represented as

$$V_D = \frac{d^3}{6} - \sum\alpha - \sum\beta \qquad [6]$$

where $\Sigma\alpha$ represents the reduction in volume due to merging along the $[01\bar{1}]$ and $[0\bar{1}1]$ directions and $\Sigma\beta$ represents the reduction in volume due to merging along the [011] and $[0\bar{1}\bar{1}]$ directions (see Appendix A: Equation [A5]), *i.e.* along the long and short domain axis. Both the charge and current density, q and j, can be calculated for an electrode using Equation [6] with the values of parameters calculated as in Appendix A.

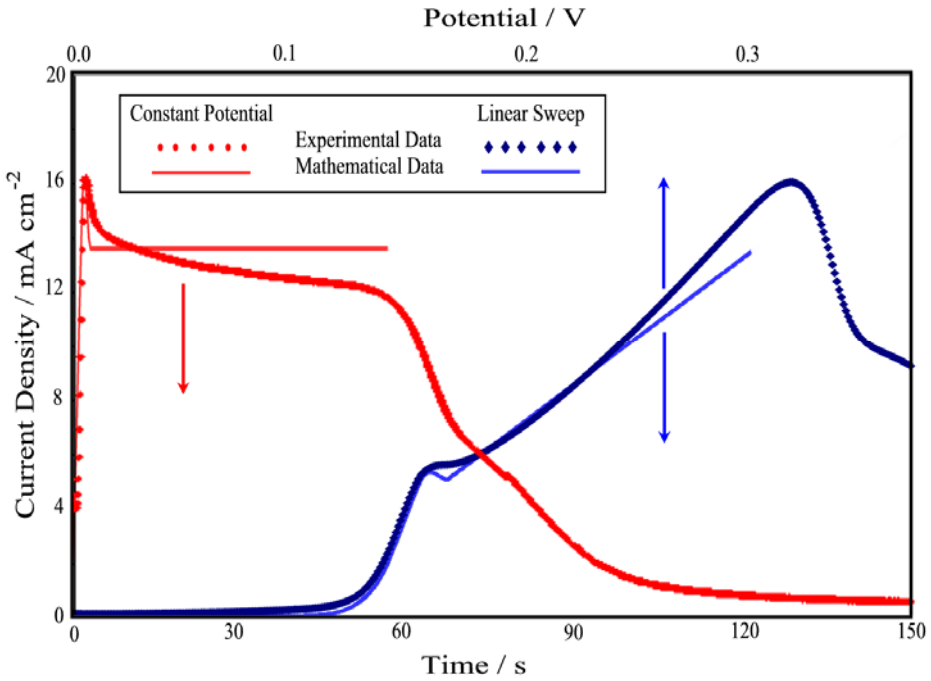


Fig. 5 Plot of the numerically-calculated (▬/▬) and experimental (●/◆) current density for both a potential-step, at a potential of 0.3 V (SCE) (▬/●), and linear sweep experiment, at a sweep rate of 2.5 mV s^{-1} (▬/◆). The experimental samples were from the same n-InP wafer ($n \approx 6.7 \times 10^{18}$ cm^{-3}). For the mathematical model a porosity of 21%, a minimum pitting potential of 0.09 V and a layer deepening rate along the $[\bar{1}00]$ direction of 25 nm s^{-1} (at 0.3 V) were used. In the potential-step model surface-pit separation along the [011] and $[01\bar{1}]$ directions were 126 nm and 90 nm, respectively, while in the case of the linear-sweep model they were 210 nm and 150 nm.

Comparison of Model to Experiment

Figure 5 shows a plot of current density versus time for a potential-step experiment, where the potential is held at 0.3 V. A plot for the current density, j, calculated by the domain merging model is also plotted on the graph for constant-potential simulation at the same potential as the experiment (using a layer deepening rate, calculated from SEM images, of 25 nm s^{-1}). The anodic peaks of the experiment and simulated data coincide; however, after the peak, the current falls off more rapidly in the simulated than in the experimental data. This may be due to there being a distribution of pit spacing in experiments and consequently domains do not all merge simultaneously. The model

assumes a regular distribution of pits that leads to simultaneous merging of all domains in both directions. The peak in current are caused by the increase in the number of active pore tips as the domains increase in volume until merging commences. After merging starts the number of active tips reduces – specifically, those at the domain surfaces that were expanding latterly and not deeper into the bulk InP decrease in number – resulting in the simulated fall-off in current. Experimentally, the plateau region that follows is not exactly horizontal and the initial fall-off in current continues for an extended duration (in comparison to the simulated data). Furthermore, there is an eventual decrease in current from this plateau that is not observed in the simulated data. The non-zero slope in the plateau region is presumably due to a slow-down in the layer growth rate (as will be discussed later) and the eventual fall-off in current is due to a cessation in the mechanism. Since the numerical model assumes a constant etching rate at the pore tips (for a constant applied potential), such decreases in current do not occur in simulations.

An LSV and simulated LPS data are also shown in Fig. 5. To simulate the LPS the current per active pore tip was assumed to be proportional to applied potential; *i.e.* the layer deepening rate was simulated to increase linearly from 0 nm s^{-1} at 0.09 V (the potential at which the current starts increasing in the LSV of Fig. 5) at a rate of 1.19 nm s^{-1} per mV (*i.e.* so that the layer deepening rate would be the same at 0.3 V as it was for the constant-potential simulation (*i.e.* 25 nm s^{-1})). Strong agreement is found between the current density of the LSV and the simulated LPS data. The first anodic peak of the simulated data, and the trough in current that follows, coincide with the respective stages in the LPS experiment. As with the potential step experiment, the current peak is narrower in the simulated data than in experiment which can be accounted for, as before, by a distribution in pit spacing and pit initiation in the experiment. However, the first anodic peak and the shape of the current curve that follows for both the LPS experiment in Fig. 5 and Fig. 2 are of very similar in shape to the simulated data; *i.e.* after the first anodic peak a trough in current is observed and the near-linear regions of the simulated and experiment data in Fig. 5 overlap. Therefore, the first current peak can be attributed to the merging of domains and the trough in current indicates the completion of domain merging (similar to the peak and initial fall-off in current in potentiostatic experiments). After the trough the current increases almost linearly since the number of active tips remains constant and the pore propagation rate (in our simulation) increases as the potential increases.

Since there is no mechanism for termination of pore propagation in the model the second anodic peak and the fall-off in current observed in experiments are not accounted for. However, the domain shape does have a significant effect on the initial current in potential-step and LPS experiments resulting in the formation of a current peak associated with domain merging and a plateau/linear region associated with the widening of a continuous porous layer. This is in agreement with the SEM observations in the previous section where domain merging coincides with the first anodic peak of the LSVs. Furthermore, these results are in agreement with LPS deconvolution experiments performed by our group, that show LPSs to be mainly time dependent during the first current peak and mainly dependent on potential during the linear region between the two peaks in current.[22] It follows that the current peak observed both in potential-step experiments and in LSVs results from merging of truncated tetrahedral domains.

In our model the linear region after the trough in current (*i.e.* after V_T) increases with potential because the number of active pore tips (during continuous porous layer deepening) is constant and our model simulates a pore propagation rate that is

proportional to the applied potential. A possible mechanism that could result in a quasi-proportional behavior between propagation rate of each pore tip and the applied potential is one where the ohmic drop between the bulk electrolyte and the electrolyte at the tip acts as a feedback mechanism that controls the rate of pore propagation. Such current (pore propagation rate) response at an individual pore tip to applied potential in its simplest form can be modeled by a resistor in series with a diode (in reverse bias). In such a model the resistor would represent the ohmic drop between the bulk electrolyte and the electrolyte at the pore tip being modeled and the diode would represent the transfer of carriers versus potential across the depletion layer at the pore tip. Once a threshold potential (the reverse break-down potential) is applied, etching can commence and current will flow. However, the flow in current will result in a potential drop across the resistor which will decrease the potential across the diode and therefore limit the current that can flow in the system. An increase in applied potential above this threshold value will result in an increase in current that, without the resistor, would increase to an avalanche current flowing through the diode (*i.e.* through the depletion layer at the pore tip). However most of the increase in potential will be across the resistor (*i.e.* across the electrolyte of the porous network) since only a small increase in potential across the diode is necessary to increase the current enough to sufficiently increase the ohmic drop across the resistor.

Equivalent Circuit for Porous Networks

In a porous domain a network of pores spread out from the domain's surface pit. This network can be modeled as a network of resistors with the same layout as the porous network with the resistor at the end of each branch of the network (*i.e.* at the tip of each pore) in series with a diode (in reverse bias). Therefore when a potential greater than the reverse break-down potential of the diodes is applied current will flow from each tip of the network back to the surface pit resulting in an ohmic drop between the tips and the surface pit. The ohmic drop across each section of the network will be proportional to the current flowing through that section. Therefore the ohmic drop becomes more and more significant the further from the tips it is, with the most significant ohmic drop occurring across the surface pit. It follows that once a continuous porous layer has been formed the region of greatest ohmic drop has already been created.

Regardless of the number of active pore tips will be more-or-less constant once such a continuous porous layer has formed (*i.e.* after the peak in current in constant-potential or LPS experiments) the ohmic drop along each pore will not be the same; that is, because the surface pit density will have increased during the initial rise in current there will be domains of porous networks of different size and therefore development (age). It follows that the tips of 'younger' domains should experience slightly higher potential than the tips of 'older' domains and, similarly, tips at the end of pores that have branched less often than their neighboring pores should experience a slightly higher potential. Therefore the tips of these 'younger' or less developed networks will propagate slightly faster than the 'older' more developed networks; in such a model the 'age' of a tip is a representation of how developed the pores connecting the tip to its surface pit are or how large the ohmic drop is between the tip and its surface pit. However, since 'older' tips propagate more slowly than 'younger' tips, the difference in 'age' will decrease with the duration of the experiment; *i.e.* 'younger' tips will out maneuver 'older' tips and therefore branch – increasing the development of their network

and the ohmic drop back to their tip – while stopping the 'older' tips from branching or propagating at all – forcing their network to 'age' less or become 'younger'.

Thus, in potentiostatic experiments, once a continuous layer has formed the plateau current region, which is flat in our simulated data, will not be flat. Instead, the current will gradually approach a quasi-steady-state as the active tips approach the same 'age': *i.e.* the ohmic drop between each tip and respective surface pit becomes the same. During this time the 'younger' tips will form more developed networks and therefore the overall current will reduce. However, once the tips have more or less the same 'age' they will branch less often and therefore the decay in current will become much less. Thus, the plateau region in potentiostatic experiments is in agreement with such a model of current response to applied potential. Furthermore, since the most significant ohmic drop occurs across the network where it was branching the most – *e.g.* the part that was etched before V_1 in the LPSs – and the 'age' of the active tips will approach the same value with time, an increase in applied potential across a continuous porous layer should result in an almost proportional increase in current at each pore tip. Therefore, the linear current region between the two current peaks in LPS experiments is also in agreement with such a model of current response.

CONCLUSIONS

A model for the expansion and merging of domains of pores into a continuous porous layer, based on truncated-tetrahedral shaped domains, was developed. The current densities for both potential-step and LPS experiments were simulated and compared with experimental data. From this investigation it was determined that the current peak in potential-step experiments and the first current peak in anodic LPS experiments correspond to the merging of porous domains with truncated-tetrahedral shapes. Furthermore the start of the plateau region in potential-step experiments and the trough in current in LPS experiments correspond to the completion of domain merging. Therefore the plateau/linear regions that follow correspond to the deepening of a continuous porous layer.

Observation by SEM of electrode surfaces after different durations of etching in LPS experiments showed that saturation of the surface-pit density occurs at the same potential as the trough in current. SEM cross-sections of the same electrodes verify the simulated result from our model, *i.e.* the first current peak is due to the merging of domains of pores with the completion of merging occurring at the potential corresponding to the trough in current. Therefore the trough in current, the formation of a continuous porous layer and the saturation of surface-pit density all occur at the same instant.

In addition, we propose that the current response at each pore tip to applied potential can be modeled by a network of resistors of the same layout as the porous network with the resistor at the end of each branch of the network connected in series with a diode (in reverse bias). In such a model the resistors represent the ohmic drops between the bulk electrolyte and the electrolyte at the pore tip and the diodes represent the transfer of carriers versus potential across the depletion layer at each of the pore tips. The behaviors of the plateau region in constant current experiments and the linear region in LPS experiments are in agreement with such a model of current response of the porous network to applied potential.

ACKNOWLEDGEMENTS

Two of the authors, R. P. Lynch and N. Quill, would like to thank the Irish Research Council for Science Engineering and Technology for postgraduate scholarships to perform this research.

REFERENCES

1. M. I. J. Beale, J. D. Benjamin, M. J. Uren, N. G. Chew, A. G. Cullis, *J. Cryst. Growth,* **73**, 622 (1985)
2. R. L. Smith and S. D. Collins, *J. Appl. Phys.*, **71**, 8 (1992)
3. M.M. Faktor, D.G. Fiddyment and M.R. Taylor, *J. Electrochem. Soc.,* **122**, 1566 (1975)
4. G. Oskam, A. Natarajan, P. C. Searson, and F. M. Ross, *Appl. Surf. Sci*., **119,** 160 (1997)
5. A.-M. Gonçalves, L. Santinacci, A. Eb, I. Gerard, C. Mathieu and A. Etcheberry, *Electrochem. Solid-State Lett.*, **10** (4), D35 (2007);
6. P. Schmuki, D.J. Lockwood, H.J. Labbé and J.W. Fraser, *Appl. Phys. Lett.,* **69**, 1620 (1996)
7. S. Langa, J. Carstensen, M. Christophersen, H. Föll, and I. M. Tiginyanu, *Appl. Phys. Lett.*, **78**, 1074 (2001)
8. P. Schmuki, J. Fraser, C. M. Vitus, M. J. Graham, H. S. Isaacs, *J. Electrochem. Soc.,* **143,** 3316 (1996)
9. P. Schmuki, D. J. Lockwood, J. Fraser, M. J. Graham, H. S. Isaacs, *Mater. Res. Soc. Symp. Proc.,* **431,** 439 (1996)
10. E. Spiecker, M. Rudel, W. Jäger, M. Leisner and H. Föll, *phys. stat. sol. (a),* **202,** 2950 (2005)
11. A. Anedda, A.Serpi, V.A. Karavanski, I.M. Tiginyanu and V.M. Ichizli, *Appl. Phys. Lett.,* **67**, 3316 (1995)
12. S. Langa, J. Carstensen, I. M. Tiginyanu, M. Christophersen, and H. Föll, *Electrochem. Solid-State Lett.*, **4**, G50 (2001)
13. S. Langa, I. M. Tiginyanu, J. Carstensen, M. Christophersen, and H. Föll, *Electrochem. Solid-State Lett.,* **3**, 514 (2000)
14. M. Christopherson, J. Cartensen, A. Feuerhake, and H. Föll, *Mater. Sci. Eng. B,* **69,** 70, 194 (2000)
15. X. G. Zhang, *J. Electrochem. Soc.,* **138**, 3750 (1991)
16. R. Lynch, C. O'Dwyer, D. Sutton, S. Newcomb, and D.N. Buckley, *ECS Trans.*, **6(2),** 355 (2007)
17. R. Lynch, C. O'Dwyer, D.N. Buckley, D. Sutton and S.B. Newcomb, *ECS Trans* **2**, 131 (2006)
18. C. O'Dwyer, D.N. Buckley, D. Sutton, M. Serantoni and S.B. Newcomb, *J. Electrochem. Soc.* **154** (2), H78 (2007)
19. C. O'Dwyer, D.N. Buckley, D. Sutton, and S.B. Newcomb, *J. Electrochem. Soc.,* **153,** G1039 (2006)
20. N. Quill, R. P. Lynch, C. O'Dwyer and D. N. Buckley, *ECS Trans.*, *this volume* (2012)
21. R. P. Lynch, M. Dornhege, P. Sánchez-Bodega, H. H. Rotermund, and D. N. Buckley, *ECS Trans.*, **6** (2), 331 (2007)

22. N. Quill, C. O'Dwyer, R. Lynch, C. Heffernan, and D. N. Buckley, *ECS Transactions* **19 (3)**, 295 (2009)

APPENDIX A

When an isolated domain merges with other domains its volume V_D can no longer expand at the same rate. The excluded volumes (*i.e.* the volumes of the regions that a domain can no longer expand into, but would have if it were an isolated domain) can be calculated from Fig. A1 as:

$$\alpha = \frac{1}{6}d_\alpha^3 \quad \text{and} \quad \beta = \frac{1}{6}h_\beta^3 + \frac{1}{2}h_\beta^2 h \qquad [A1]$$

where α and β represent the excluded volumes along the [01$\bar{1}$] and [011] directions respectively.

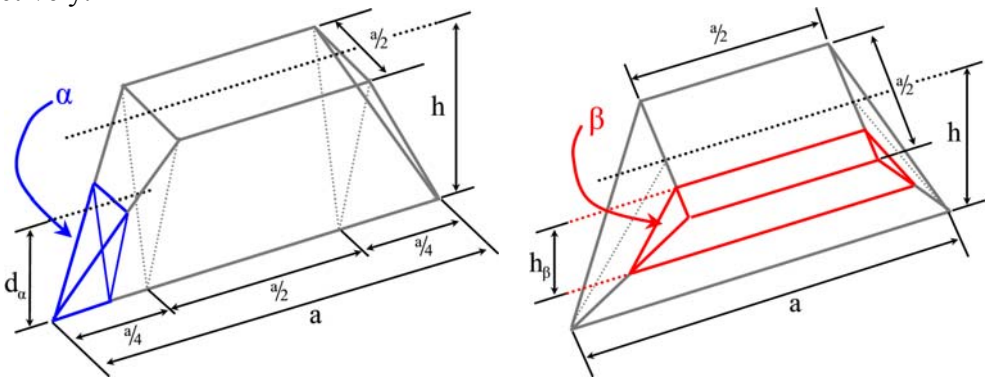


Fig. A1 Schematics are shown of isolated domains of depth h. (a) The region marked α represents the excluded volume (*i.e.* the volume the domain is was unable to expand into due to merging with another domain) along the [01$\bar{1}$] direction (b) while the region marked β represents the exclude volume along the [011] direction.

Eventually the regions, α and β, overlap on another or, in the case of α, extend outside of the electrode surface and where this happens adjustments must be made to α and β to calculate a corrected V_D.

Fig. A2(a) shows a situation where α extends past the electrode-surface and therefore must be corrected by a volume X.

$$X = \frac{1}{2}(d_\alpha - h)^2\left[h + \frac{d_\alpha - h}{3}\right] \qquad [A2]$$

Fig. A2(b) shows an example of how the volumes of α and β can overlap. It follows that a correction Y can be made to either α or β:

$$Y = \frac{1}{12}(d_\alpha + h_\beta - h)^3 - Z \qquad [A3]$$

where Z is a correction to Y in the situation where α extends past the electrode-surface as shown in Fig. A2(c):

$$Z = \frac{1}{4}(d_\alpha - h)^2\left[\frac{1}{3}(d_\alpha - h) + h_\beta\right] \qquad [A4]$$

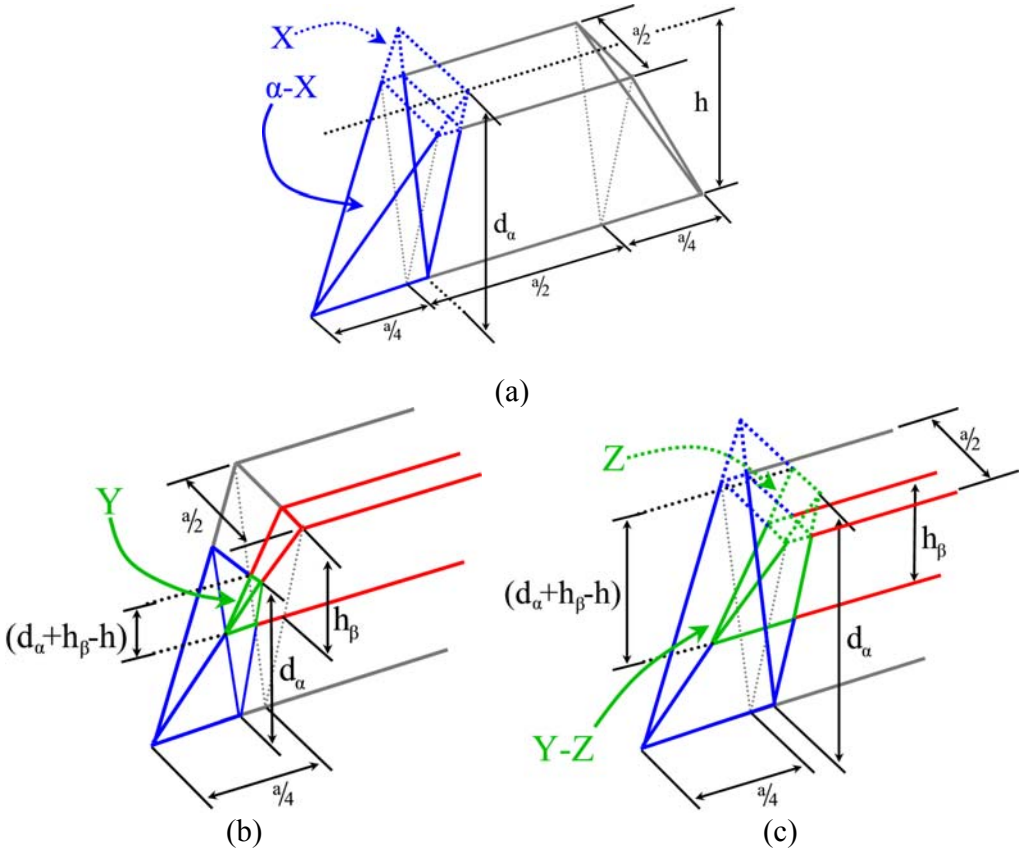


Fig. A2 Schematics of an individual domains of depth h (a) where the region marked α (representing the excluded volume along the [01$\bar{1}$] direction; see Fig. A1(a)) is overestimated by a volume X; (b) where α and β (representing the excluded volume along the [011] direction; see Fig. A1(b)) overlap by a volume Y and (c) where α extends past the electrode-surface resulting in Y extending past the surface (and therefore outside of β) by a volume Z.

Once these adjustments are made the domain volume V_D can be calculated during merging and from this both the charge and current densities, q and j, can be calculated for an electrode. It follows that the volume of the average domain can be calculated as follows:

$$\begin{aligned} V_D &= \frac{d^3}{6} - \sum\alpha - \sum\beta \\ \alpha &= \frac{1}{6}d_\alpha^3 - X \\ \beta &= \frac{1}{6}h_\beta^3 + \frac{1}{3}h_\beta^2 h - Y \\ X &= \frac{1}{2}(d_\alpha - h)^2\left[h + \frac{d_\alpha - h}{3}\right] \\ Y &= \frac{1}{12}(d_\alpha + h_\beta - h)^3 - Z \end{aligned} \qquad \text{[A5]}$$

$$Z = \frac{1}{4}\left(d_\alpha - h\right)^2\left[\frac{1}{3}\left(d_\alpha - h\right) + h_\beta\right]$$

where $\Sigma\alpha$ represents the reduction in volume due to merging along the $[01\bar{1}]$ and $[0\bar{1}1]$ directions and $\Sigma\beta$ represents the reduction in volume due to merging along the [011] and $[0\bar{1}\bar{1}]$ directions.